arXiv:1405.7238v2 [physics.acc-ph] 9 Jun 2014

High Power Fibre Laser System for a High Repetition Rate Laserwire

L. J. Nevay,* R. Walczak, and L. Corner
John Adams Institute at the University of Oxford,
Denys Wilkinson Building, Keble Road, Oxford, OX1 3RH United Kingdom
(Dated: June 10, 2014)

We present the development of a high power fibre laser system to investigate its suitability for use in a transverse electron beam profile monitor i.e. a laserwire. A system capable of producing individual pulses up to 165.8 ± 0.4 μJ at 1036 nm with a full-width at half-maximum of 1.92 ± 0.12 ps at 6.49 MHz is demonstrated using a master oscillator power amplifier design with a final amplification stage in a rod-type photonic crystal fibre. The pulses are produced in trains of 1 ms in a novel burst mode amplification scheme to match the bunch pattern of the charged particles in an accelerator. This method allows pulse energies up to an order of magnitude greater than the steady-state value of 17.0 ± 0.6 μJ to be achieved at the beginning of the burst with a demonstrated peak power of 25.8 ± 1.7 MW after compression. The system is also shown to demonstrate excellent spatial quality with an $M^2 = 1.26 \pm 0.01$ in both dimensions which would allow nearly diffraction limited focussing to be achieved.

PACS numbers: 07.60.Vg, 42.60.By, 29.27.Fh

I. INTRODUCTION

For a future linear electron-positron collider such as the International Linear Collider (ILC) [1] and the Compact Linear Collider (CLIC) [2], the generation and transport of beams while preserving the low emittance is essential to achieve the required final focus beam sizes and therefore high luminosity. This requires measurement, monitoring and control of the transverse beam emittance along the entire accelerator chain, preferably in a non-invasive manner. In a linear accelerator, one possible method of measuring the emittance is by measuring the transverse size of the beam at several points in the lattice with different betatron phases. Two methods to achieve this are wire-scanners that measure a projection of the beam and optical transition radiation (OTR) screens to image the beam directly [3], but these can both suffer damage from high charge density beams. Conventional methods such as these are disruptive to the beam and they cannot be used for measurement and tuning of the accelerator during operation, therefore the development of new diagnostics is essential.

A laserwire is a beam size diagnostic in which a tightly focussed laser beam is scanned perpendicularly across an electron beam [4]. A small fraction of the laser photons undergo Compton-scattering, resulting in electrons with degraded energies and high energy photons that travel nearly parallel to the electron beam. A dipole magnet further along the accelerator separates these from the primary electron beam as shown in Figure 1. The Compton-scattered photons can be detected further along the beam line after a bending magnet where the photons and electrons are separated. Alternatively, in the case of a high energy collider ($E_e > 50$ GeV), the energy of the electrons is degraded by a large fraction and it would be possible to detect these electrons as they are lost from the lattice. Both can be used as a measure of the Compton-scattering rate, which is modulated as the laser focus is scanned transversely across the electron beam, providing a laserwire scan. With knowledge of the laser size at its focus, the scan can be deconvolved to yield the electron beam size [5].

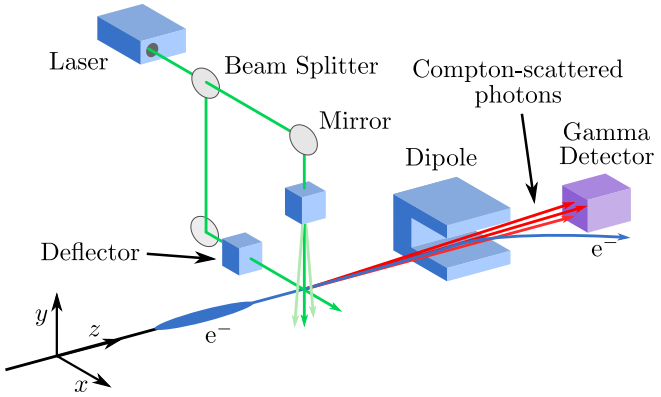

FIG. 1. Conceptual schematic of a laserwire. A laser beam is scanned perpendicularly to an electron beam producing Compton-scattered photons that are detected after a dipole magnet.

For accurate determination of the electron beam size, the laser spot size must be of a similar or ideally smaller size than the electron beam. The laser must be of sufficient intensity to produce a detectable number of Compton-scattered photons relative to the detector background environment. Furthermore, it must have the excellent spatial beam quality required to create the focussed spot sizes of approximately a micrometre that will be required for use in a laserwire, at the ILC or CLIC. If a pulsed laser source is used, it must also have pulses of a similar duration to that of the individual electron

* laurie.nevay@rhul.ac.uk; now at Royal Holloway, University of London

bunches for optimal laser-electron collision luminosity, which would for example imply a pulse duration of approximately 1 ps for the ILC.

High power commercially available lasers typically emit light in the near infrared. As diffraction limits the achievable focussed spot size to approximately the wavelength of the light, it is necessary to convert the laser light to a shorter wavelength to produce the small beam sizes required for a laserwire. However, light with a wavelength shorter than 300 nm experiences strong absorption in most optical materials necessitating reflective focussing optics rather than transmissive ones. A laserwire at the Stanford Linear Collider (SLC) demonstrated micrometre-size scans with sub-micrometre resolution using an ultraviolet laser with a reflective focussing geometry [6, 7]. This geometry prevents direct measurement of the laser focus and therefore calibration as well as imposing a very short scanning range due to the optical aberrations incurred when the focussing mirror is used off-axis - for example when either the laser or the mirror is moved to scan the focussed laser spot across the electron beam. Transmissive optics afford a much greater scanning range and allow direct measurement of the focussed spot size. Given these advantages, a compromise is to use a visible wavelength generated by frequency doubling a near infrared source, which increases the resolution but reduces the peak power [8].

Apart from the laserwire at SLC, several other laserwires have been demonstrated. A laserwire at PETRA-III in DESY [9] using a commercial Q-switched pulsed laser at 20 Hz made laserwire scans of $\sigma \sim 30$ μm on electron bunches in a ring acclerator with a precision of 5 %. An installation at the damping ring of the Accelerator Test Facility 2 (ATF2) used a continuous-wave laser with cavity enhancement to measure an electron beam size of 9.8 μm [10]. Here, the very low Compton-scattering rate from the low power laser is balanced by the megahertz revolution frequency of the electron bunches in the ring. In these cases, the low repetition rate and low average laser power respectively preclude fast intra-train scanning as would be required at the ILC. Another laserwire installation at the linear extraction line of ATF2 has shown micrometre-sized scans using a gigawatt peak power Q-switched pulsed laser at 3.25 Hz [11]. Despite the high resolution and signal level at this installation, the low repetition rate of the laser system also prevents intra-train scanning. In each case, the laser technology limits the usability of the laserwire as a diagnostic for a future linear collider.

In this paper, we consider the requirements for a laserwire at the ILC and present the results of a fibre laser system developed for use there. Its suitability is demonstrated through the calculation of the yield of Compton-scattered photons for such a system at the ILC.

TABLE I. Nominal ILC BDS electron beam parameters.

Parameter	Symbol	Value	Units
Beam Energy	E	250	GeV
Normalised horizontal emittance	ϵ_x^*	10	μm rad
Normalised vertical emittance	ϵ_y^*	40	nm rad
Train repetition frequency	f_{train}	5	Hz
Number of bunches per train	N_{train}	1312	
Bunch repetition frequency	f_{bunch}	1.81	MHz
Bunch duration	$\sigma_{\tau e}$	1	ps
Number of electrons per bunch	N_e	2×10^{10}	

II. ILC LASERWIRE SPECIFICATIONS

The ILC is a proposed linear collider that is intended to collide electrons and positrons initially at 250 GeV and eventually up to 500 GeV. Such a machine is needed to make precision studies of the recently discovered Higgs boson and to investigate potential new discoveries at the Large Hadron Collider at CERN and will require ∼20 laserwires in various locations as a primary accelerator diagnostic [1]. Laserwires will be of crucial importance in the beam delivery system (BDS) after the main linac, where precise measurements of the electron beam size of the order of a micrometre are necessary to ensure that the electron and positron beams can be focussed to the required nanometre sizes at the interaction point. The parameters of the electron beam in the ILC BDS are shown in Table I.

The luminosity of the laser photon and electron collision is linearly proportional to both the number of photons and the number of electrons as well as the cross-section for the interaction, which in this case is the Compton cross-section. Agapov *et al.* [5] have shown that given typical detector efficiencies and operational experience of a laserwire, a wavelength of 532 nm, laser pulse length of $\sigma_\tau = 1$ ps and focussed to a size of $\sigma_l = 1$ μm, that a laser peak power of approximately 10 MW will be required for each of the laserwires planned for use in the ILC. Currently available commercial laser systems capable of this peak power can do so only at kilohertz repetition rates and typically have a low overall efficiency. Such a system would therefore preclude intra-train scanning at megahertz repetition rates, and given the low electron bunch train repetition rate of 5 Hz, would take much longer to achieve the required measurement precision. In the case of a future linear collider, the emittance measurement system may be used often for continuous feedback and tuning purposes and a system utilising intra-train scanning would decrease the measurement time as well as increase the precision. Additionally, the spatial quality of such laser systems can be unsuitable for achieving the necessary diffraction-limited focussed spot sizes.

A peak power of 10 MW with a pulse length of 1 ps corresponds to an energy of 10 μJ per pulse. High energy

ultrashort laser pulses in the visible part of the spectrum are typically produced by frequency doubling a source at $\lambda \sim 1$ μm, which can be achieved with an efficiency of 60 % [12]. Therefore, pulses of ~ 17 μJ in the near infrared are required at the megahertz repetition rate to allow intra-train scanning of the electron bunches.

III. FIBRE LASER

A technology with great potential for laserwires and other accelerator applications is that of optical fibre lasers, which has progressed rapidly in recent years, allowing the efficient generation of high energy ultrashort pulses [13]. The waveguide structure of optical fibres means they have excellent spatial quality and high efficiency due to the long interaction lengths with the pump sources. However, high intensities that arise in the small core diameters of single mode step-index fibres can induce optical nonlinearities that affect the spectral and temporal properties of the output pulses and limit the maximum useful output [14]. One solution to this problem has been the development of photonic crystal fibres (PCFs) that have large mode areas with nearly single mode spatial output that allow high energy pulse extraction [15]. In particular, rod-type PCFs have the largest core diameters that can be up to 100 μm [16] and have been shown to produce 1 mJ, 800 fs output pulses at 100 kHz [17]. Rod-type PCFs cannot be connectorised like normal optical fibres, but they are desirable as their large area allows the highest peak powers to be achieved without optical nonlinearities. Fibre lasers have excellent conversion of pump to laser light and in addition, are pumped by highly efficient diode sources leading to very high overall wall plug efficiency. This, together with the excellent spatial quality and reliability of fibre lasers make them attractive for applications such as laserwire.

To investigate the suitability of a fibre laser for a laserwire, a system was developed consisting of a commercial chirped pulse amplification (CPA) fibre laser followed by further amplification in an 80 cm long Yb-doped rod-type PCF (NKT Photonics DC-200/85-Yb-ROD). The commercial laser (Amplitude Systèmes) consists of a Yb:KYW oscillator at 1036 nm producing 19 nJ pulses at 51.92 MHz, locked to a Rb stabilised external radio frequency signal generator. The 500 fs oscillator pulses are stretched to $\sim$200 ps and then the repetition rate reduced to 6.49 MHz by an acousto-optic modulator. The pulses (now 6 nJ) are amplified in two stages in Yb-doped 25 μm core diameter fibre and then pass through an electro-optic modulator (EOM) for macropulse shaping, producing ~ 1.5 μJ output pulses in bursts as short as 500 ns, which are used as a seed for the PCF.

The PCF has a core diameter of 85 μm to guide the seed, an inner cladding diameter of 200 μm to guide the pump, and an outer cladding diameter of 1.7 mm. The 400 W, 976 nm pump diode laser (Newport Spectra-Physics) is coupled into the PCF in a counter propagating geometry allowing independent optimisation of both the seed and the pump coupling as well as increased efficiency [18]. Fused silica endcaps 8 mm long and 10 mm diameter at both ends of the fibre allow the unguided light from the core and inner-cladding to expand before exiting through the glass air interface, reducing the possibility of damage to the fibre [19]. The seed and pump are separated by dichroic mirrors at either end of the PCF, which is made entirely of silica with no polymer coating and is supported in a metal V-groove. Due to the high efficiency of fibre lasers and the large surface area to volume ratio, the fibre requires neither active nor passive cooling. The experimental arrangement is shown in Figure 2.

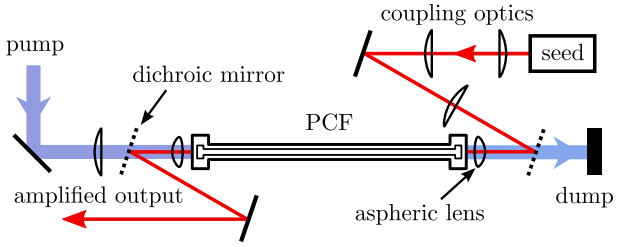

FIG. 2. Experimental arrangement for amplification in a PCF with coupling and decoupling aspheric lenses as well as dichroic mirrors to separate the pump and seed beams.

A. Burst Mode Amplification

Whilst high peak power laser pulses are required at megahertz repetition rates to match the electron beam for intra-train scanning, the bunch trains have a low duty cycle (0.4 %). The laser system was matched to produce pulses with a similar duty cycle, significantly reducing the average power and therefore cooling requirements as well as avoiding wasting laser energy when there are no electron bunches. The EOM in the seed laser allows the necessary macropulse shaping and the pump output is modulated using the output of a signal generator as a gate to the power supply.

Simultaneously starting both the pump and the seed will not result in a uniform burst of amplified pulses as the pump has a finite rise time ($\sim$100 μs). With a simultaneous start, the PCF will not be pumped initially and the Yb dopant will absorb the incoming seed due to its quasi-three-level nature. During the rise time of the pump, the PCF becomes first transparent and then amplifies the seed. By turning on the pump before the seed by approximately the rise time of the pump a more uniform output can be achieved. However, by further increasing the delay of the seed burst with respect to the pump the Yb dopant is pumped without the seed depleting its excited upper-state population and energy can be stored in the PCF resulting in higher gain during the seed burst. After approximately the upper state lifetime

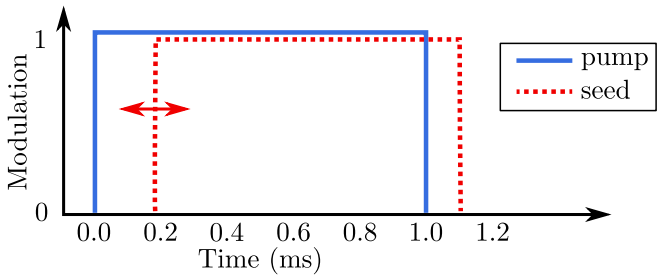

FIG. 3. Modulation envelopes of the seed and pump laser for burst operation with the pump preceding the seed for high gain.

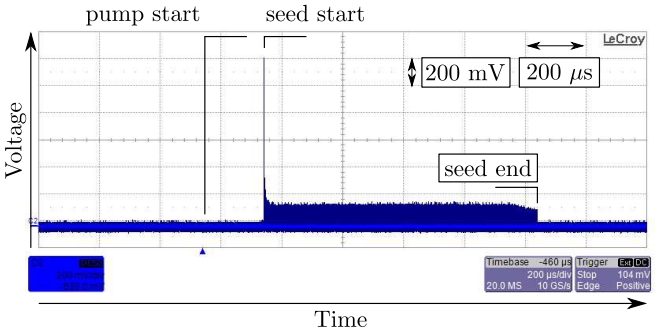

FIG. 4. Oscilloscope screenshot showing a 20 mega-sample photodiode trace of the amplified output exhibiting exponential decay of pulse energies to a steady-state level. The high number of pulses in the ∼1 ms burst results in a solid trace when viewed on this timescale and the aliasing of the oscilloscope displays a much larger degree of noise than is actually present.

of Yb in glass (0.8 ms), spontaneous emission of the excited population will reduce the available gain and may lead to large laser pulses oscillating in the rod that can lead to catastrophic damage [20].

An investigation was carried out to characterise this process and in doing so a method was demonstrated by which pulses almost an order of magnitude greater in energy than the steady-state can be achieved. The pump laser requires a minimum operation time of 1 ms, which corresponds to ∼6500 pulses of the seed. Initially, the seed and pump bursts were operated simultaneously and then the start of the seed burst was delayed with respect to the start of the pump as shown in Figure 3. As the pump laser also has a finite fall time and some excited upper-state population still exists even when the pump is turned off, the seed burst was extended by 100 μs beyond the end of the pump to safely extract the stored energy. The system was operated at 2 Hz due to the limitation of the energy meter used to integrate the energy of the full burst and the system is capable of operating at higher burst repetition rates.

As this technique relies on a build up of gain beyond the normal steady-state, it is to be expected that the high repetition rate seed pulses will deplete the upper-state population before it is replenished by the pump. Consequently, the initial pulses in the burst will experience a very high gain with subsequent pulses experiencing decreasing gain until the steady-state is reached. Although it is possible to compensate for this by modulating the incoming seed train before the PCF, this is still an active area of research, and can lead to lower individual pulse energies in the burst [21]. Despite the lack of uniformity in pulse energies, this scheme serves to investigate the potential output from a fibre laser and could also be compensated for by pulse energy normalisation in a laserwire system.

B. Characterisation

To characterise the output of the laser system, the pulse energies, spatial quality and temporal profiles were measured. The megahertz repetition rate of the pulses presents many practical challenges for conventional techniques used to measure these aspects of the pulses on an individual basis.

1. *Pulse Energies*

The amplified seed burst from the PCF with a seed delay relative to the pump of 0.13 ms is depicted in a photodiode trace in Figure 4, which shows a high initial series of pulses that rapidly decay to a steady-state level. As the pulses vary in energy significantly they cannot be assumed to be same and must be measured individually. The megahertz repetition rate is beyond the ability of the fastest commercially available energy meters to discriminate individual pulses. Therefore, an energy meter capable of measuring the energy of the total burst (Gentec QE25-SM-LP) was used in combination with a digitised trace of a fast (< 35 ps rise time) photodiode (Newport 818-BB-25 InGaAs) to resolve the individual pulse energies. As the peak of the photodiode pulses is proportional to the laser pulse energy, the digitised photodiode signal can be used to subdivide the total energy of the burst. The energy of a given pulse in the burst is therefore given by

$$E_{(i)} = \left(\frac{E_{total}}{\Sigma_i V_{peak(i)}} \right) V_{peak(i)} \qquad (1)$$

where $E_{(i)}$ and $V_{peak(i)}$ are the pulse energy and peak voltage of ith pulse respectively, and E_{total} is the total energy of the burst. An oscilloscope with a high bandwidth, sample rate and sample memory was used (LeCroy WaveRunner 402-MXi) to digitise the photodiode trace of the total burst with 12 bit precision at 10 giga-samples s^{-1}. Two Fresnel beam splitters were used with several neutral density filters to reduce the intensity of the pulses to within the measured linear range

of the photodiode and 10 waveforms recorded for statistical purposes.

For the most accurate measurement of the pulse energies in the seed burst, the photodiode traces were recorded using two different scalings on the oscilloscope; firstly with a scaling such that the high voltage peaks of the initial laser pulses were sampled properly; and secondly scaled so that the initial pulses were clipped but the majority of the burst was digitised with a higher precision. This method of using two combined sets of photodiode traces reduces the uncertainty in the calculated pulse energy from approximately 20 % to 1 %, which is due to the sum of the peak voltage of several thousand pulses. Additionally, the extension of the seed beyond the pump was chosen to give a discrete end to the pulse train making the number of pulses in the burst clearly identifiable.

The pump level was increased until sharp spikes appeared in the amplified spectrum - a sign of the presence of amplified spontaneous emission (ASE) and an indication that additional pump energy would not produce further useful amplified output. The incident pump burst energy was 297 ± 1 mJ and the input seed burst energy was 6.43 ± 0.02 mJ, which corresponds to an input pulse energy of 0.95 ± 0.01 μJ. A seed delay of 200 μs was found to give the maximum pulse energy of the first amplified pulse and in this case the total energy of the output amplified seed burst was 100.1 ± 0.2 mJ. The output burst energy along with the digitised photodiode traces was used to calculate the pulse energies of the 5842 pulses shown in Figure 5. These show a maximum pulse energy of 165.8 ± 0.4 μJ with an exponential decay in pulse energy to a steady-state. The mean pulse energy from pulse number 200 to 5000 is 17.0 ± 0.6 μJ with a pulse to pulse variation of 0.5 %. The linear decrease in pulse energy at the end of the pulse train is indicative of the pump turn off and depletion of gain in the PCF. The high initial pulse energies and following exponential decay are shown more clearly in Figure 6, which shows the first 35 pulses.

To investigate the relationship between the delay of the seed burst with respect to the pump pulse and the energy of the first pulse in the amplified seed burst, the seed delay was varied from 0 to 200 μs and the pulse energies of the full burst measured. The energy of the first pulse in the burst as a function of seed burst delay is shown in Figure 7.

With the simultaneous start of the seed and pump, the energy of the first pulse in the output burst was 0.71 ± 0.01 μJ, which is lower than the incident pulse energy from the seed of 0.95 ± 0.01 μJ. At a seed delay of 200 μs, the gain of the initial pulse was 27.2 ± 0.1 dB m^{-1}.

The long term stability of the laser system was observed by making energy measurements over several periods of up to 12 hours, over which a variation of $< 1\%$ was observed.

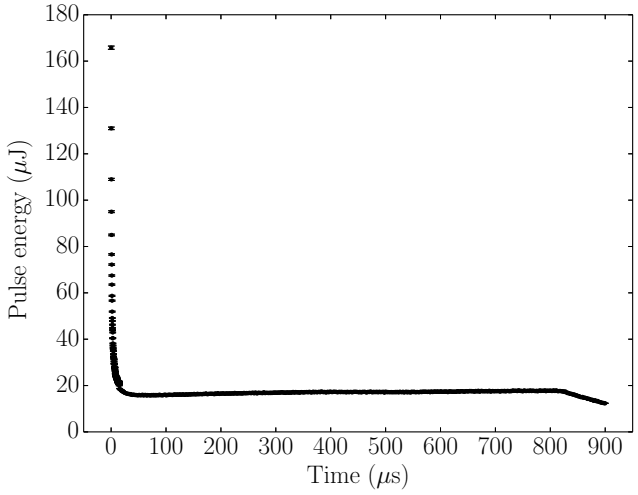

FIG. 5. Amplified pulse energies for a seed delay of 200 μs relative to the pump.

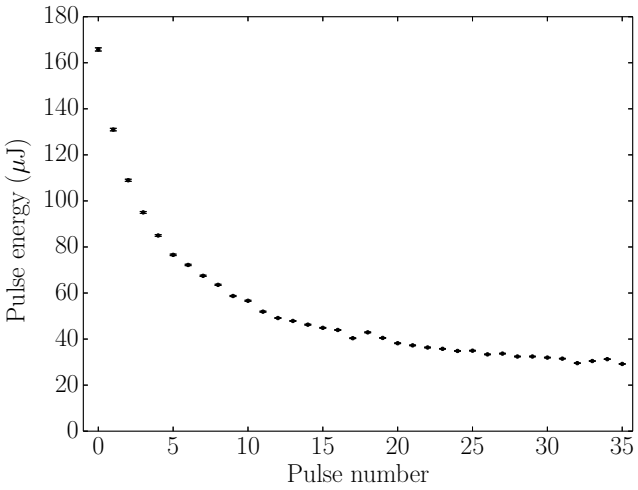

FIG. 6. Amplified pulse energies at the beginning of the seed burst shown in Figure 5.

2. Spatial Quality

The spatial quality was measured by focussing the maximum amplified output beam from the PCF using an $f = 1$ m plano-convex lens. A laser beam profiler on a translation stage was used to measure the transverse profile at several points throughout the focus. The 4σ diameter of the laser beam as it propagates can then be modelled by comparing it to a perfect Gaussian mode using the M^2 model [22]. The M^2 parameter of the laser beam then linearly scales the focussed spot size for a given input beam size to a lens and its focal length, with a perfect Gaussian by definition having an M^2 of 1. The 4σ diameters and the M^2 model fits are shown in Figure 8 with measured values of $M_x^2 = M_y^2 = 1.26 \pm 0.01$. This excellent spatial quality is well suited for creating diffraction limited focussed spot sizes.

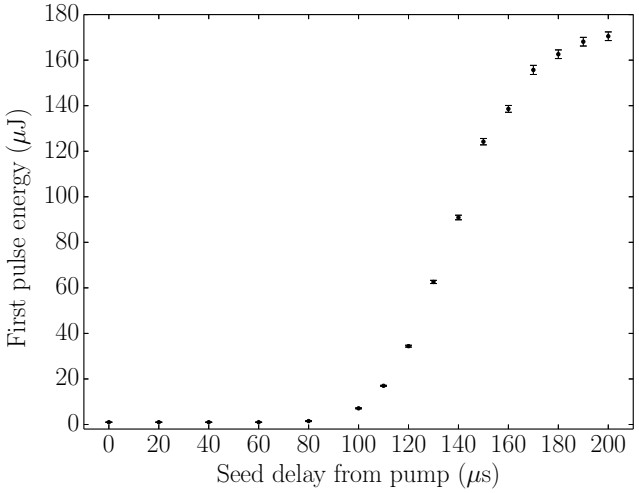

FIG. 7. Energy of the first pulse in the amplified train for various seed burst delays relative to the pump burst.

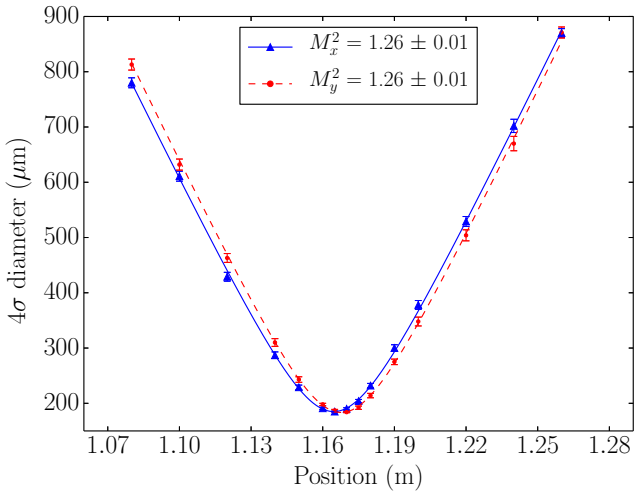

FIG. 8. M^2 measurement of amplified seed pulses with both the x and y fits shown.

3. *Pulse Duration*

In a CPA laser system the pulses are temporally stretched before amplification to avoid optical nonlinearities as well as damage to the amplifier and compressed back to their original duration afterwards. The stretcher introduces linear group delay dispersion (second order phase) to the pulse, stretching it in time, and the compressor is designed to compensate for this as well as any higher order phase terms accumulated by the pulse during amplification. However, dispersion caused by nonlinear effects such as self-phase modulation cannot necessarily be corrected and in this case the compressed pulse will have a different temporal profile and duration to the initial pulse. Although high peak powers can be achieved in optical fibre amplifiers, the presence of nonlinearities limits the compression and therefore the final peak power attainable. It is therefore important to measure the compressed pulse duration.

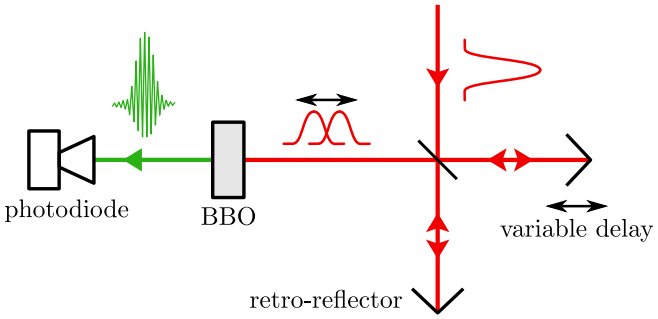

FIG. 9. Schematic of an autocorrelator, consisting of an interferometer with beam splitter, retro-reflectors, a variable delay arm, BBO crystal and photodiode.

Ultrashort laser pulses well below 1 ns cannot be characterised by electronic devices alone as their response is too slow and therefore another technique must be used. Optical autocorrelation is the most common way of measuring these pulse durations [23] and therefore an autocorrelator based on a scanning Michelson interferometer was used for our pulse duration measurement. This consists of a 50:50 beam splitter to split the incoming pulse, two retro-reflectors to recombine the split pulses at the beam splitter and a beta-Barium Borate (β-BaB_2O_4, BBO) frequency doubling crystal to analyse the interference between the two pulses as shown in Figure 9. One arm of the interferometer is mounted on a translation stage and as it is scanned the delay between the two pulses is varied. The resultant frequency doubled output as detected by a photodiode shows the interference fringes, the envelope of which is the convolution of the pulse with itself. The standard technique involves scanning one arm of the interferometer and continuously recording data. In our case however, the low duty cycle of the bursts and the significant time taken to digitise the waveforms makes this implementation unsuitable. Instead, waveforms were recorded at a series of static positions and the setup was mechanically agitated during the data recording, allowing the envelope to be observed at that position. A large number of waveforms were recorded at each position to ensure the full extent of the envelope was captured. To deconvolve the autocorrelation an assumption about the temporal profile of the pulse is required. We assume a Gaussian temporal profile with a deconvolution factor of $\sqrt{2}$.

For verification, we compared pulse duration measurements made with both the method described above and also the conventional scanning autocorrelation technique. To perform this comparison, the EOM was turned off so that the laser output consisted of a series of continuous pulses rather than operating in a burst mode. This enabled us to take data using both methods that could be directly compared. The conventional scanning autocorrelation is shown in Figure 10. The upper en-

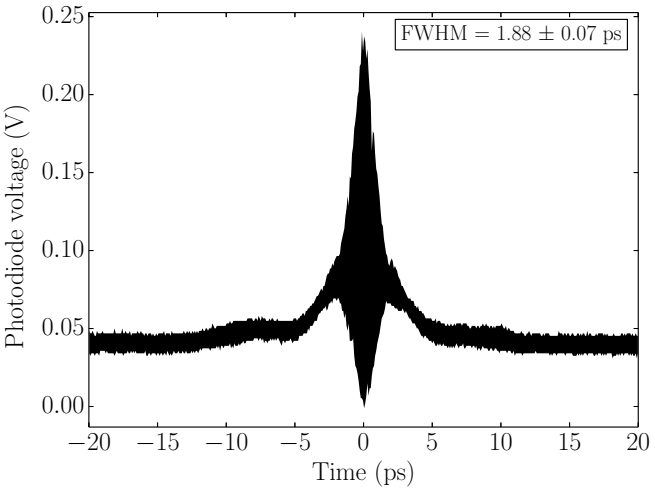

FIG. 10. Autocorrelation of the seed laser compressed without transmission through the final PCF amplification stage.

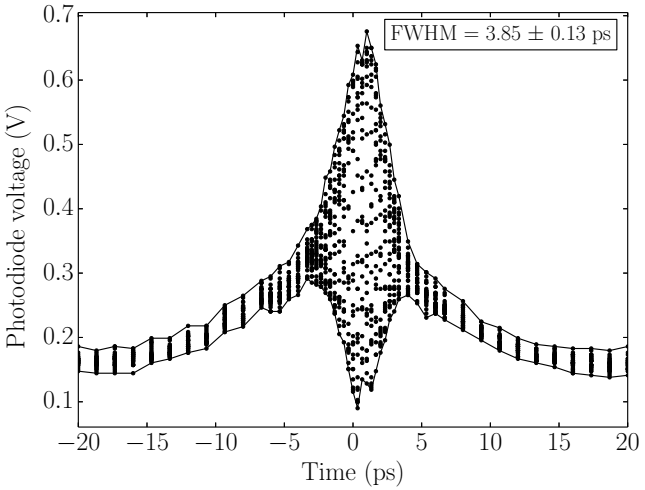

FIG. 12. Autocorrelation of the unamplified compressed seed pulses transmitted through the PCF.

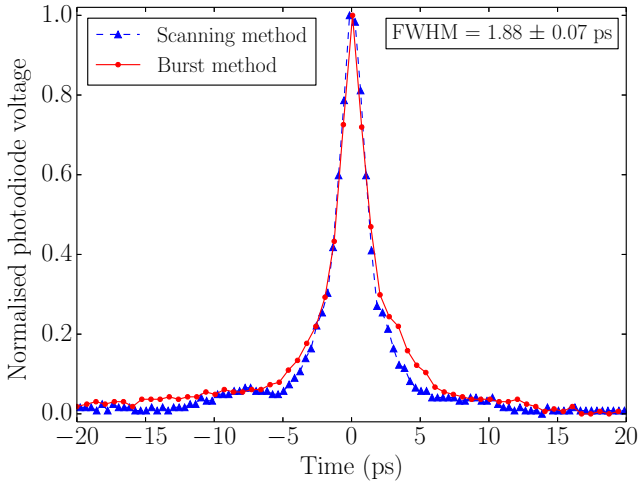

FIG. 11. Envelope of autocorrelations of the seed laser made using both the conventional scanning method and the burst operation method showing good agreement with identical FWHM.

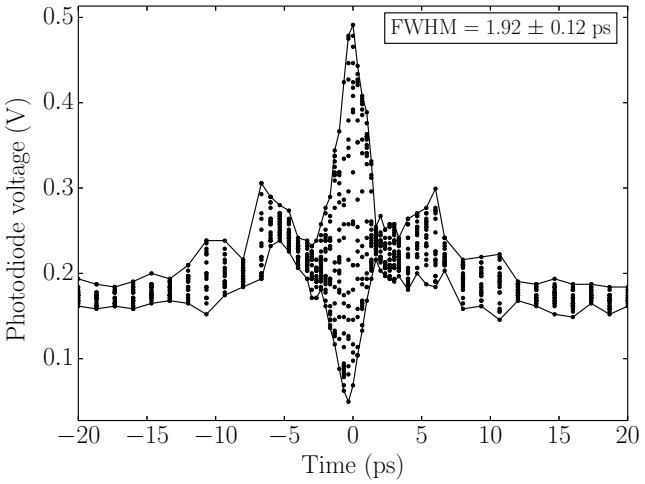

FIG. 13. Autocorrelation of the first pulse in the amplified burst with an energy of 165.8 ± 0.4 μJ with the envelope shown.

velopes of this autocorrelation and that of the autocorrelation performed in burst mode are shown together in Figure 11 and show excellent agreement between both methods with a deconvolved full-width at half-maximum (FWHM) of 1.88 ± 0.07 ps in both cases. This is also indicative of the achievable pulse durations possible from this seed laser used with the PCF.

Having measured the compressed output of the commercial system before the PCF, we then measured the effect of transmission through the PCF both with and without amplification. The autocorrelation of the unamplified compressed output from the PCF is shown in Figure 12, which shows a slightly wider peak with a deconvolved FWHM of 3.85 ± 0.13 ps as well as slight wings. The transmission through the PCF introduces additional dispersion to the pulse that could not be fully compensated for by the compressor of the commercial laser used in this research, which has a fixed layout and a transmission efficiency of 75 %.

Figure 13 shows the autocorrelation of the first pulse in the amplified burst with the highest energy and therefore the most likely to have generated optical nonlinearities. In this case, only a small fraction of the amplified output from the PCF was compressed to avoid damage to the commercial compressor. The autocorrelation shows a more complicated structure than the previous autocorrelations with a narrow peak with a FWHM of 1.92 ± 0.12 ps as well as double wings on either side. Again, the fixed compressor arrangement prevents the possible compensation of additional dispersion introduced by the amplification. The wings in the autocorrelation indicate a temporal structure beyond a simple Gaussian such as a pre or post pulse [24]. The

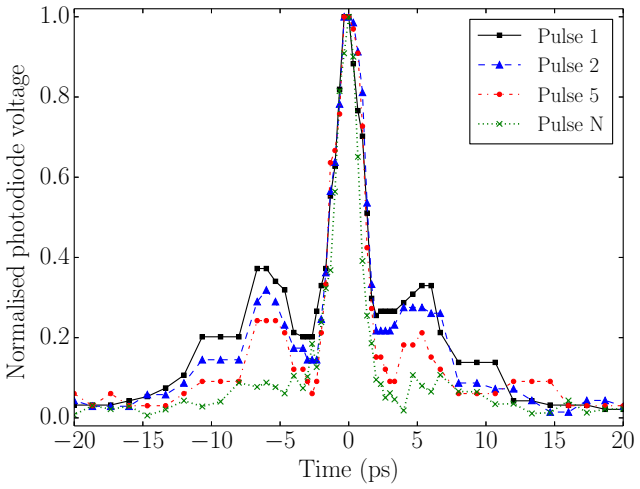

FIG. 14. Autocorrelation envelopes of pulses 1, 2, 5 and the *nth* pulse, which is a pulse much later in the burst that is in the steady state. Each is normalised showing a clear reduction in the wings as the pulse energy decreases.

central peak, as defined by the minima on either side, accounts for 40 ± 1 % of the total area of the autocorrelation and therefore that percentage of the total pulse energy is contained within the central peak. With the initial pulse energy of 165.8 ± 0.4 μJ, and the compressor transmission of 75 %, the peak power is correspondingly 25.8 ± 1.7 MW. The normalised upper envelopes of the autocorrelations of this and subsequent pulses are shown in Figure 14.

It can be seen that for pulses further into the train, the wings are smaller in the autocorrelations and a higher percentage of the pulse energy is contained within the central peak. As the pulses are also decreasing in energy, this would indicate an intensity dependence consistent with the presence of optical nonlinearities. The peak powers calculated from the percentage of energy in the central peak and the pulse durations are shown in Table II. These peak powers would be significantly enhanced by the use of a compressor properly designed to compensate for the phase accumulated in the PCF amplifier.

4. *Polarisation*

As discussed in Section I, the infrared laser source must be frequency doubled to the visible part of the spectrum to achieve a smaller focussed spot size. Frequency conversion requires that the input source be highly linearly polarised. Optical fibres do not preserve the polarisation of an input source due to inhomogeneities and stresses on the fibre caused by bending and torsion along its length. However, unlike most optical fibres the rod-type PCF is straight and therefore these effects were expected to be minimal.

The degree of linear polarisation (DOLP) was measured by recording the transmitted power through a polarising beam splitter as a function of angle and the maximum, P_{max} and minimum, P_{min} transmitted powers are used to determine the DOLP using Equation 2.

$$\text{DOLP}\,(\%) = 100 \times \left(\frac{P_{max} - P_{min}}{P_{max} + P_{min}}\right) \tag{2}$$

The DOLP of the input seed was measured to be 96.4 ± 0.4 % and the DOLP of the amplified output was 95.3 ± 0.3 %. This shows that the output is linearly polarised and that amplification in the PCF did not affect the polarisation despite the lack of specific polarisation maintaining structure.

5. *Pointing Stability*

The laser system for a laserwire cannot not be placed next to the accelerator beam line directly due to the damaging high radiation environment. Furthermore, this placement would preclude access to the laser system for maintenance. Therefore, the laser system must be located in a separate area from the particle accelerator and the laser beam transported to the laserwire stations by either a system of mirrors (free-space transport) or in fibre. With the required peak powers, it is not currently possible to transport laser pulses in fibre without incurring optical nonlinearities that would distort the temporal and spectral properties of the laser pulse.

Under free-space propagation, the pointing stability of the laser must be considered as the angular jitter of the laser beam produces spatial jitter of the laser profile at the laserwire lens. As many laser pulses are required to make a laserwire scan, the corresponding spatial jitter of the focussed laser beam is therefore convolved with the transverse size of the electron beam and increases the measured transverse size.

The pointing stability of the laser system was measured by measuring the laser profile centroid of the collimated output laser beam using a high resolution CCD beam profiler at a distance of 3.518 m, where the laser beam size (4σ) was measured to be 8.157 ± 0.022 mm. The standard deviation of the centroid was meaured over a 20 min period to be 3.820 μm, which corresponds to an angular jitter of 1.09 ± 0.03 μrad. For a laserwire system at a distance of 20 m [25] producing a 1 μm focussed spot size using this laser beam, the spatial jitter at the focus would be < 10 nm. When convolved with the laserwire scan this contribution would be negligible. At a greater distance, the contribution may be non-negligible, but measurable and can be subtracted in analysis.

TABLE II. Summary of the measured properties and calculated peak powers of the pulses using the compressor transmission efficiency of 75 %. The *nth* pulse is representative of the mean of the steady-state pulses. The number of interacting photons ($N_{\gamma\ \mathrm{interacting}}$) was calculated by calculating the proportion of the total pulse energy within the full-width at half-maximum (FWHM) of the central peak. This was scaled assuming 75 % compressor transmission and 60 % frequency doubling efficiency. The number of Compton-scattered photons is calculated from this assuming ILC electron beam parameters detailed in Section IV for two possible laserwire collision angles of $\pi/2$ and $\pi/6$.

Pulse #	Energy	FWHM	Central Peak	Peak Power	$N_{\gamma\ \mathrm{interacting}}$	$N_C\,(\theta=\pi/2)$	$N_C\,(\theta=\pi/6)$
	μJ	ps	%	MW			
1	165.8 ± 0.4	1.92 ± 0.12	40	25.8 ± 1.7	7.8×10^{13}	8496	22495
2	131.0 ± 0.4	1.89 ± 0.12	40	20.8 ± 1.4	6.1×10^{13}	6755	17884
3	109.0 ± 0.4	1.82 ± 0.11	41	18.5 ± 1.2	5.2×10^{13}	5845	15472
4	95.1 ± 0.3	1.72 ± 0.11	45	18.6 ± 1.3	5.0×10^{13}	5712	15118
5	84.9 ± 0.3	1.75 ± 0.11	54	19.9 ± 1.4	5.4×10^{13}	6082	16099
nth	17.0 ± 0.1	1.73 ± 0.11	100	7.4 ± 0.5	2.0×10^{13}	2265	5994

IV. APPLICATION AS A LASERWIRE

In order to assess the suitability of the developed laser system for a laserwire, the yield of Compton-scattered photons from a laser pulse with an electron bunch must be considered along with the detector efficiency and required precision. Reviews of luminosity calculations and Compton-scattering cross-sections are given in [4, 26] and a brief summary is given here.

The number of Compton-scattered photons is given by the product of the luminosity $L(\theta)$ and the compton cross-section $\sigma_C(\omega)$, which are dependent on the collision angle [27, 28]. The Compton cross-section is given by the product of the Thomson cross-section ($\sigma_T = 0.665 \times 10^{-28}\ \mathrm{m}^2$) with $f(\omega)$, which is given by

$$f(\omega) = \frac{3}{4}\left\{\frac{1+\omega}{\omega^3}\left[\frac{2\omega(1+\omega)}{1+2\omega} - \ln(1+2\omega)\right] + \frac{\ln(1+2\omega)}{2\omega} - \frac{1+3\omega}{(1+2\omega)^2}\right\} \quad (3)$$

where ω is the normalised energy of the laser photons in the electron rest frame, is given by

$$\omega = \frac{hE_b}{\lambda c^3 m_e^2}(1+\cos\theta) \quad (4)$$

Here, λ is the laser wavelength and E_b the electron beam energy (h is the Planck constant, c the speed of light and m_e the electron mass). The luminosity $L(\theta)$ can be decomposed into the product of the luminosity for a head on collision $L(0)$ and a reduction factor $R(\theta)$

$$L(0) = \frac{n_\gamma\, n_e}{2\pi\sqrt{\sigma_{\gamma x}^2+\sigma_{ex}^2}\sqrt{\sigma_{\gamma y}^2+\sigma_{ey}^2}} \quad (5)$$

$$R(\theta) = \frac{1}{\sqrt{1+\left(\frac{\sigma_{\gamma z}^2+\sigma_{ez}^2}{\sigma_{\gamma x}^2+\sigma_{ex}^2}\right)\tan^2(\theta/2)}} \quad (6)$$

where n_γ and n_e are the number of photons in the laser pulse and electrons in a bunch respectively. The laser pulse and electron bunch are assumed to have Gaussian distributions with the corresponding sigma parameters in three orthogonal dimensions; $\sigma_{\gamma x}$, $\sigma_{\gamma y}$, $\sigma_{\gamma z}$ and σ_{ex}, σ_{ey}, σ_{ez} respectively. For simplicity, the laser divergence is neglected, i.e. it is assumed that the Rayleigh range of the laser is large compared to σ_{ex}.

Taking the ILC as an example, representative parameters of the electron beam in the BDS part of the accelerator where a laserwire is likely to be used are $E_b = 250$ GeV, $n_e = 2 \times 10^{10}$, $\sigma_{ex} = 10\ \mu$m, $\sigma_{ey} = 1\ \mu$m and $\sigma_{ez} = 300\ \mu$m [5]. Assuming 75 % transmission through a laser compressor, 60 % frequency-doubling conversion efficiency ($\lambda = 518$ nm), the measured pulse energies from the laser system described are used to estimate the number of Compton-scattered photons for collision angles of both $\pi/2$ and $\pi/6$ as summarised in Table II. Only the pulse energy within the central peak of the laser pulse is considered.

The collision angle of $\pi/6$ in the horizontal plane increases the luminosity but effectively reduces the distance over which the laser beam diverges across the electron beam. With the electron beam sizes mentioned, the reduced Rayleigh range is still over double the width of the electron beam. Even when present, such effects do not preclude the use of a laserwire as has been recently shown [25].

Assuming a detector efficiency of 5 % [5], the number of detected Compton-scattered photons from the highest

energy pulse with an angle of $\pi/2$ would be 425, which is enough for a good electron beam emittance measurement [5]. With an angle of $\pi/6$, this is increased to 1125 detected photons, which would significantly improve the detector statistical accuracy. Using the steady state pulse energy at this angle, 300 photons would be detected, which is still adequate for a laserwire at the ILC.

V. CONCLUSIONS & OUTLOOK

A fibre laser system suitable for an ILC laserwire has been demonstrated. Using a novel burst mode amplification regime, pulses an order of magnitude greater in energy than achievable in the steady-state have been shown with a maximum pulse energy of 165.8 ± 0.4 μJ. This method was shown to be controllable by varying the relative timing of the pump and the seed bursts allowing a range of initial pulse energies. The methods developed to characterise the 6.49 MHz pulses were detailed, which allowed measurement of the pulse energy and autocorrelation on a pulse by pulse basis. The spatial quality of the amplified laser output was measured and shown to be excellent, which would allow small focussed spot sizes to be achieved.

The demonstrated high peak powers could be further improved with a specifically designed compressor that properly compensates for the additional group delay dispersion introduced in the PCF to produce shorter duration pulses and consequently higher peak powers. In this case, the useful pulse energy within the pulse duration would be significantly increased from 40 % demonstrated in the highest energy pulse. Furthermore, stretching the oscillator pulses to approximately 1 ns is possible and would significantly reduce the nonlinearities accumulated. Research on better compression and more efficient gain extraction in the PCF is underway.

Regarding the use of the laser for a laserwire diagnostic, the system described would currently be suitable for use with the ILC and if required, averaging of multiple electron bunches would decrease the uncertainty of the measurement. The demonstrated laser pulse train varies significantly in pulse energy with an initial pulse approximately an order of magnitude greater than the steady state. Normalisation could be used to account for this variation as the pattern was found to be very stable. Whilst the steady state pulse energies are sufficient, it may be highly desirable to have a different operational mode for a laserwire where a small number of high energy pulses can be generated allowing alignment or calibration.

The background conditions for such an accelerator have yet to be accurately simulated and this is an active area of research. With this information, the required laser pulse energy could be more precisely defined. Simulation of the laserwire signal in combination with the accelerator backgrounds is also highly relevant as although laserwire diagnostics have been demonstrated at test facilities, the high energy case of the ILC will provide multi-GeV Compton-scattered photons that may be more distinguishable from background sources than those at the lower energy test facilities. In addition, improvement of the detector efficiency would have a significant impact on the required laser peak power.

This system demonstrates the peak powers required for a laserwire diagnostic as well as excellent spatial quality, which in addition to the high electrical efficiency of fibre lasers demonstrates their suitability for accelerator applications.

ACKNOWLEDGMENTS

The research leading to these results has received funding from the Science and Technology Facilities Council via the John Adams Institute, University of Oxford and CERN.

[1] C. Adolphsen, M. Barone, B. Barish, K. Buesser, P. Burrows, *et al.*, *The International Linear Collider Technical Design Report - Volume 3.II: Accelerator Baseline Design*, Tech. Rep. (2013).

[2] M. Aicheler, P. Burrows, M. Draper, T. Garvey, P. Lebrun, K. Peach, and N. Phinney, *A Multi-TeV Linear Collider Based on CLIC Technology: CLIC Conceptual Design Report*, Tech. Rep. (2012).

[3] D. Brandt, *CERN Accelerator School: Course on Beam Diagnostics*, Tech. Rep. (CERN, Geneva, 2009).

[4] P. Tenenbaum and T. Shintake, Annu. Rev. Nucl. Phys. **49**, 125 (1999).

[5] I. Agapov, G. Blair, and M. Woodley, Phys. Rev. ST Accel. Beams **10**, 112801 (2007).

[6] R. Alley, D. Arnett, E. Bong, W. Colocho, J. Frisch, S. Horton-Smith, W. Inman, K. Jobe, T. Kotseroglou, D. McCormick, J. Nelson, M. Scheeff, S. Wagner, and M. Ross, Nucl. Instrum. Methods A **379**, 363 (1996).

[7] M. Ross, in *Particle Accelerator Conference*, Vol. 1 (2003) pp. 503–507 Vol.1.

[8] S. Boogert, G. Blair, G. Boorman, A. Bosco, L. Deacon, P. Karataev, A. Aryshev, M. Fukuda, N. Terunuma, J. Urakawa, L. Corner, N. Delerue, B. Foster, D. Howell, M. Newman, R. Senanayake, R. Walczak, and F. Ganaway, Phys. Rev. ST Accel. Beams **13**, 122801 (2010).

[9] T. Aumeyr, G. Blair, S. Boogert, G. Boorman, A. Bosco, K. Balewski, E. Elsen, V. Gharibyan, G. Kube, S. Schreiber, and K. Wittenburg, in *IPAC MOPE069* (Kyoto, Japan, 2010).

[10] H. Sakai, Y. Honda, N. Sasao, S. Araki, Y. Higashi, T. Okugi, T. Taniguchi, J. Urakawa, and M. Takano, Phys. Rev. ST Accel. Beams **4**, 022801 (2001).

[11] L. Nevay, G. Blair, S. Boogert, P. Karataev, K. Kruchinin, L. Corner, and R. Walczak, in *IPAC MOPWA053* (Shanghai, China, 2013).

[12] J. Rothhardt, T. Eidam, S. Hädrich, F. Jansen, F. Stutzki, T. Gottschall, T. V. Andersen, J. Limpert, and A. Tünnermann, Opt. Lett. **36**, 316 (2011).

[13] D. J. Richardson, J. Nilsson, and W. A. Clarkson, J. Opt. Soc. Am. B **27**, B63 (2010).

[14] J. Limpert, R. Fabian, D. N. Schimpf, E. Seise, T. Eidam, H. Steffen, and J. Rothhardt, IEEE J. Quantum Electronics **15**, 159 (2009).

[15] J. Limpert, N. Deguil-Robin, I. Manek-Hönninger, F. Salin, F. Röser, A. Liem, T. Schreiber, S. Nolte, H. Zellmer, A. Tünnermann, J. Broeng, A. Petersson, and C. Jakobsen, Opt. Expr. **13**, 1055 (2005).

[16] C. D. Brooks and F. Di Teodoro, Appl. Phys. Lett. **89**, 111119 (2006).

[17] F. Röser, T. Eidam, J. Rothhardt, O. Schmidt, D. N. Schimpf, J. Limpert, and A. Tünnermann, Opt. Lett. **32**, 3495 (2007).

[18] D. Xue, Q. Lou, and J. Zhou, Optics & Laser Technology **39**, 871 (2007).

[19] J. W. Dawson, M. J. Messerly, R. J. Beach, M. Y. Shverdin, E. A. Stappaerts, A. K. Sridharan, P. H. Pax, J. E. Heebner, C. W. Siders, and C. Barty, Opt. Expr. **16**, 13240 (2008).

[20] J. Limpert, N. Deguil-Robin, S. Petit, I. Manek-Hönninger, F. Salin, P. Rigail, C. Hönninger, and E. Mottay, Appl. Phys. B **81**, 19 (2005).

[21] S. Breitkopf, A. Klenke, T. Gottschall, H. J. Otto, C. Jauregui, J. Limpert, and A. Tünnermann, Opt. Lett. **37**, 5169 (2012).

[22] T. Johnston, Appl. Opt. **37**, 4840 (1998).

[23] A. Monmayrant, S. Weber, and B. Chatel, J. Phys. B **43**, 103001 (2010).

[24] R. Trebino, C. C. Hayden, A. M. Johnson, W. M. Simpson, and A. M. Levine, Opt. Lett. **15**, 1079 (1990).

[25] L. Nevay, S. Boogert, *et al.*, "Laserwire at the Accelerator Test Facility 2 with Sub-Micrometre Resolution," (2014), arXiv:1404.0294 [physics.acc-ph].

[26] T. Suzuki, *General Formulas of Luminosity for Various Types of Colliding Beam Machines*, Tech. Rep. KEK-76-3 (KEK, 1976).

[27] O. Klein and Y. Nishina, Z. Phys. **52**, 853 (1929).

[28] Y. Miyahara, Nucl. Instrum. Methods A **588**, 323 (2008).